Jpn. J. Appl. Phys. Vol. 40 (2001) pp. 4340–4343
Part 1, No. 6B, June 2001

In-Situ Electrical Study of a Reversible Surface Modification and a Nanomachining of Gold Microstrips by the Voltage-Biased Atomic Force Microscope Tip in Air

Byong Man KIM*, Yo-Sep MIN, Nae Sung LEE†, Jung Hyun SOK, Moon Kyung KIM, Soo Doo CHAE, Won Il RYU and Hee Soon CHAE

Material and Device Laboratory, Samsung Advanced Institute of Technology, San #14, Nongseo-Ri, Kiheung-Eup, Yongin-City, Kyungki-Do 449-900 Korea

(Received January 16, 2001; revised manuscript received April 13, 2001; accepted for publication April 16, 2001)

We report on a reversible polymerization of ambient carbonaceous deposits on the surface of gold microstrips by means of a voltage-biased atomic force microscope tip in air. This approach is found capable of controlled writing, erasing, and rewriting of carbon-rich deposits with sizes in nanometer regime. Physical mechanism for this reversible patterning is proposed to be the current-induced electrochemical process. In addition, we introduce a novel nanomachining technique based on an electric field enhanced cutting process.

KEYWORDS: polymerization, carbon, gold microstrip, atomic force microscopy, electrochemistry

1. Introduction

It is well known that exposure of a surface to an electron beam radiation in vacuum or air can lead to the formation of contamination film on the exposed area. This contamination film is conceived to be produced through electron beam induced polymerization of organic molecules that are adsorbed onto the surface. The sources of these organic molecules may include residual gas molecules such as hydrocarbon and carbon dioxide in ambient or vacuum environment and layers adsorbed onto the surface during sample preparation.

The use of focused electron beams generated from the tip of scanning tunneling microscope (STM) or secondary electron microscope (SEM) in vacuum has been shown to be effective in producing well-defined contamination deposits with nanometer sizes on the surface of films including gold, silicon, and silicon dioxide.[1)] Contamination deposits produced by these means have been used in a variety of applications such as an etch mask or a high resolution atomic force microscope lithography and imaging.[2)] However, none of these studies were aimed at the erasing and rewriting of contamination deposits generated by electron beam.

In this study, we tested the possibility of using the voltage-biased atomic force microscope (AFM) tip as a patterning tool for writing and erasing of contamination features on the surface of gold microstrip in ambient condition and as a tool for rewritable data storage. We provide evidences that it is possible to reversibly polymerize ambient gas species with nanometer scale controllability and that the mechanism underlying the reversible patterning is an electrochemical process. In addition, we demonstrate a novel nanomachning technique by presenting the *in-situ* electrical data representing the time evolution of reduction in conducting cross section caused by removal of gold layers by an electric field enhanced cutting and a load-force induced ploughing process.

2. Experimental

We used photolithography and liftoff using a commercially available photoresist (AZ 5214E) to pattern 20-nm-thick evaporated Au films on a 300-nm-thick SiO_2 thermally grown on a Si(100) wafer. The SiO_2/Si wafers were treated with the standard RCA cleaning prior to the microfabrication. Each microfabricated gold pattern is consisted of a 10-μm-wide strip and connected to large gold contact pads. After gold evaporation (with a 1 nm of Ti sublayer evaporation for better adhesion) in a chamber under 10^{-8} Torr, the gold microstrips were transferred by liftoff using 10 min submerging in a 70°C striping solution (n-methyl pyrrolidinone) followed by 2-min rinse in flowing de-ionized water and N_2 blow dry. The samples were then mounted in a chip carrier, wire bonded and loaded to a commercial AFM (Park Scientific Instruments, AUTOPROBE M5) system so that the electrical measurements could be made *in-situ* while performing AFM patterning. AFM patterning and imaging were done under ambient conditions (with a relative humidity of $\sim$45% at 25°C) using a contact-mode AFM equipped with 30 nm Ti-coated commercial Si cantilevers. Unless otherwise stated, all AFM measurements in this study were made using the load force of 10.9 nN and the z-feedback loop activated. In the following, voltages are quoted with the polarity of the tip side. The sample is grounded and the constant or sweeping voltage is applied to the tip. The samples are imaged with the same tip both before and after applying voltages.

3. Results and Discussion

3.1 AFM nanostructuring and in-situ electrical characterization

By applying a negative voltage up to ~ -12 V to a fixed or a moving tip, a mound or a raised line was produced on a microfabricated gold surface. We remark that no deposit of any kind was observable on a pristine gold film by using positive tip polarity. Figure 1(a) shows an AFM image of several mounds produced over a sweeping voltage range of -4 V and -12 V. As visible in the figure, this process rendered mounds in the size range 0.1 μm–0.5 μm in diameter and 4 nm–11 nm high. In contrast to the report by Mamin *et al.*[3)] where a threshold of $\sim$3.5 V was observed for the mound formation under the field of a STM tip, we did not see a sharp threshold for the technique presented here. The threshold amplitude at which a given tip begins to produce mounds varied from

*Author to whom correspondence should be addressed. E-mail address: bmkim@sait.samsung.co.kr
†FED Project Team.

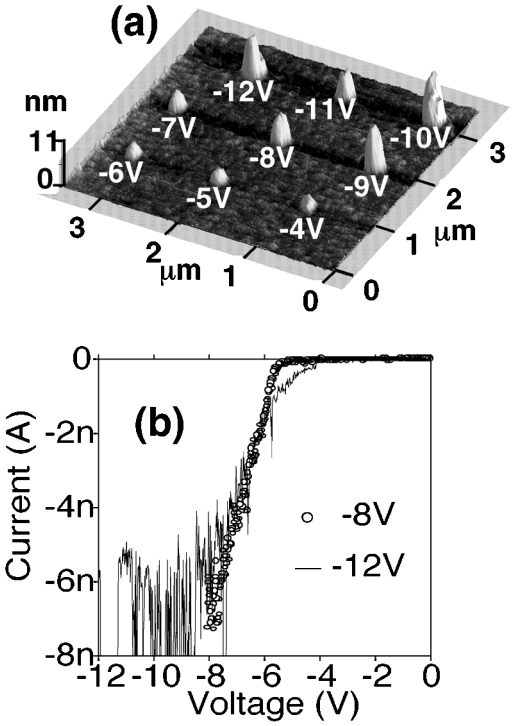

Fig. 1. AFM image of several mounds produced over a sweeping voltage range of -4 and -12 V. (b) Two I–V curves obtained by measuring current flowing to the AFM tip while applying sweeping voltages from 0 to -8 V and -12 V, respectively, during patterning two of the mounds in (a).

under -3 to -9 V. Such a threshold behavior is illustrated in Fig. 1(b), which shows a typical current-voltage characteristic across the tip-sample junction during AFM patterning. The I–V curves in Fig. 1(b) were obtained by measuring a current flowing to the tip while applying sweeping voltages from 0 to -8 V and -12 V, respectively, during pattering two of the mounds in Fig. 1(a). We confirmed that a threshold voltage for a rapid current increases, such as the one seen around -5 V in Fig. 1(b), marks the initiation of a mound formation. This observation provides evidence that the mound formation on the surface of gold microstrips requires a current flow between the underlying surface and the voltage-biased AFM tip.

We were also able to create raised lines on the surface of gold microstrips using multiple passes of a negatively biased scanning tip. Figure 2 shows a set of such lines produced over a constant voltage range of -4– -8 V with -2 V incremental step. The measured line width and height over this voltage range is between 80 nm–300 nm and 3 nm–15 nm, respectively. Note that the probability of mound or line formation increases with increasing negative voltage. The observed

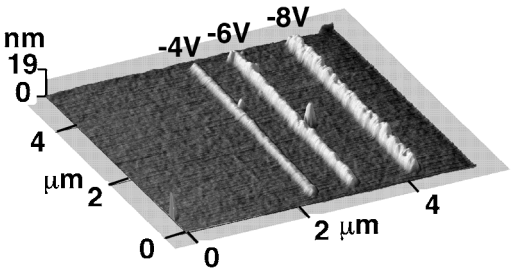

Fig. 2. AFM image of a set of raised lines produced over a constant voltage range of -4– -8 V with -2 V incremental step.

size dependencies on the amplitude and the polarity of applied voltages indicate that a possible mechanism underlying the AFM patterning is an electrochemical process.

Applying tip voltages beyond -12 V is found effective in creating depressions of varying size and shape in the Au film. An example of such depression in the shape of trench, which was produced by applying the -19 V biased tip scanning across the Au microstrip at a rate of 5 μm/s, is shown in Fig. 3(a). The height profile reveals that the trench is about 0.2 μm wide and 20 nm deep from the microstrip surface. The time evolution of the microstrip conductance (G-t) in Fig. 3(b) recorded while producing the trench in Fig. 3(a) exhibits that the conductance drops below the current detection limit of 1 pA within 2 s of applying the -19 V tip bias. Figure 3(c) shows an AFM image of a trench which was manufactured without applying any voltage bias to the scanning tip while maintaining the z-feedback loop deactivated and the load force increased above $\sim 1\,\mu$N. The G-t curve of Fig. 3(d) recorded while producing the trench in Fig. 3(c) shows that the conductance decreases gradually in a stepwise fashion below the current detection limit of 1 pA in 20 s of the AFM scanning.

We think that the conductance decreases shown in Figs. 3(b) and 3(d) represent the time evolution of reduction in conducting cross section caused by removal of gold layers by an electric field enhanced cutting and a load-force induced ploughing process, respectively. In the case of an electric field enhanced cutting process, the debris is found only and stick strongly along the edges of the trench. While in the case of a load-force induced ploughing process, the debris is observed to accumulate and stick relatively loosely both at the ends and along the edges of trench. This indicates that the nanomachning mechanism is quite different for the two cases. The former process may involve a concurrent occurrence of an electrical heating and a load-force dependent scratching, whereas for the latter case the load-force dependent scratching is a sole cause for material removal. In addition, it can be seen from the comparison of G-t curves of Figs. 3(b) and 3(d) that it takes about 8 times longer period for scribing the trench in Fig. 3(c) than the one seen in Fig. 3(a). This implies that applying -19 V to the tip is effective in generating an electrostatically induced load force in excess of $\sim 8\,\mu$N exerted on the sample surface, since a load force of above $\sim 1\,\mu$N was used for scribing the trench of Fig. 3(c).

3.2 Compositional analysis

To better elucidate the physical mechanism, we analyzed the composition of patterned features with micro-Auger spectroscopy. Figure 4(b) shows a typical SEM image of a patterned feature. The $\sim 2\,\mu\text{m} \times 4\,\mu$m pattern in Fig. 4(b) was created by moving a -7 V tip orthogonal to a scan direction at a rate of 1um/s during patterning. As shown in the figure, patterned areas typically appeared much darker under SEM inspection that resembled contamination from background hydrocarbons. Auger electron spectroscopy measurements on the patterns revealed that the patterns are compositionally enriched with carbon. The spectra of P1 and P2 in Fig. 4(a) were obtained from the patterned surface indicated respectively by P1 and P2 in Fig. 4(b). The spectra P3 and P4 in Fig. 4(a) were obtained from the pristine Au surface indicated by P3 and P4 in Fig. 4(b). In both spectra, Au signal peaks at ~ 150

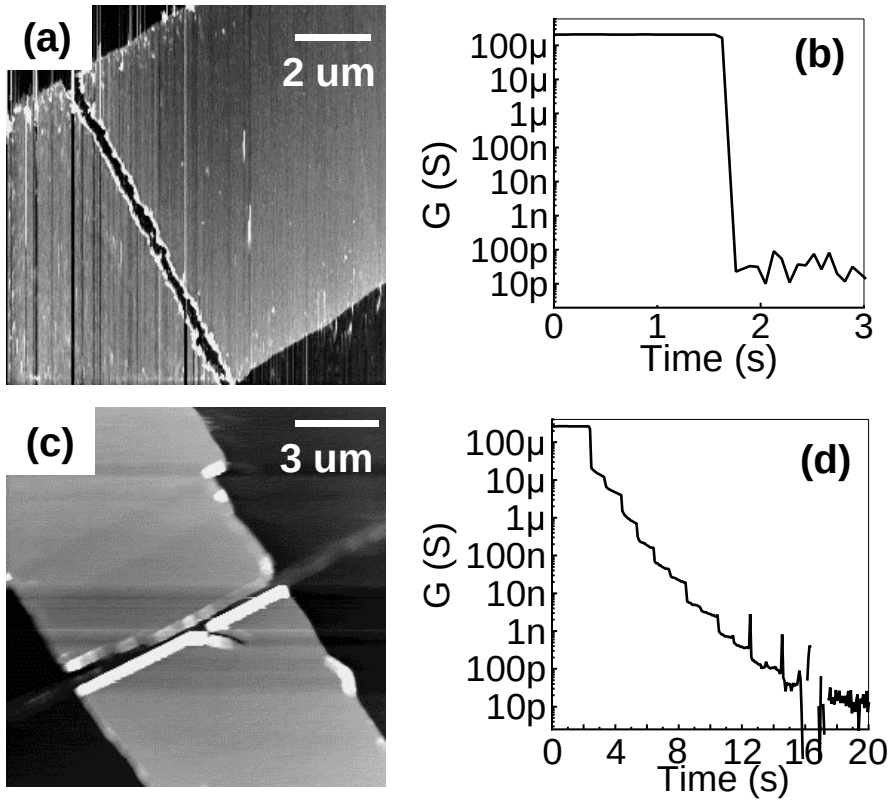

Fig. 3. (a) AFM image of a trench produced by applying the -19 V biased scanning tip across the Au strip. (b) The time evolution of the strip conductance (G-t) recorded while producing the trench in (a). (c) AFM image of a trench produced without applying any voltage bias to the scanning tip across the Au strip while maintaining the z-feedback loop deactivated and the load force increased above $\sim 1\,\mu$N. (d) G-t curve recorded while producing the trench in (c).

and carbon signal peak at ~ 280 can be seen. However, the gold peak intensity in spectra P1 and P2 is significantly reduced in comparison to that in spectra P3 and P4, since in region P1 and P2, the signal from the pristine surface of gold microstrip was masked by the carbon-rich feature produced via AFM patterning. The carbon detected away from the patterned site is likely due to the contamination during sample preparation and as it was exposed to room air for several days before Auger could be done.

3.3 Reversible polymerization

The applicability of this technique for rewritable storage is demonstrated in Fig. 5. Shown in Fig. 5(a) is a $2\,\mu\text{m} \times 3\,\mu\text{m}$ pattern written with a -6 V tip scanning at $1\,\mu$m/s. The patterned area appears to be bright in the AFM image. It is noteworthy that the unpatterned area away from the carbon deposit exhibits a granular morphology of gold whereas such granularity is absent in the patterned area. By applying a $+5$ V stationary tip for 5 s over nine spots in the central region of the carbon feature in Fig. 5(a), we were able to erase a section of a $0.5\,\mu\text{m} \times 0.7\,\mu\text{m}$ rectangular area as shown in Fig. 5(b). The granularity is revealed in the surface of the erased area. To get an information for how small an area can be erased, we applied a $+5$ V stationary tip for 5 s over three additional spots in the upper portion of the carbon deposit. This erasing sequence gave rise to three holes with the sizes in the range 100 nm diameter and 10 nm depth (Fig. 5(c)). Figure 5(d) is a result of a rewriting sequence where a 80 nm wide and 5 nm high mound was created with -6 V stationary tip applied for 5 s on a point in the center of the rectangularly erased area. This sort of reversible patterning could be repeated for many times using a same tip without losing its ability for AFM imaging. Based on these findings, we surmise that a likely mechanism underlying the local erasing of carbon features is a current induced electrochemical dissociation and/or desorption of carbonaceous deposits.

Our interpretation that current induced chemical reaction occurring in the presence of ambient organic molecules may explain some previously reported results on STM surface and ballistic electron emission microscopy (BEEM). In particular, Hasegawa *et al.*,[4] using combined STM and BEEM in air, reported that a layered structure or facetted planes appeared on a clean gold surface over the modified interface area by the attempted modification process. And, the features appeared on the clean gold surface disappeared concurrently with the recovery of the modified interface area. They have suggested vacancy formation or charging effect at the interface as possible origins for the reversible modification at the interface. They have not considered the reversible deposition of organic molecules on the gold surface as a possible cause for a reversible contrast seen in BEEM current image. This will be especially applicable if the deposition on the surface induced by the STM/BEEM modification process is composed of electrically less conductive material than gold. While other alternative explanations such as a field evaporation and desorbtion of atoms transferred from tip to surface or surface to tip are possible, a current-induced electrochemical deposition and dissociation of ambient carbon-rich film is an attractive picture to explain our observed reversible results. However, it is also likely in our work that the surface of gold microstrips

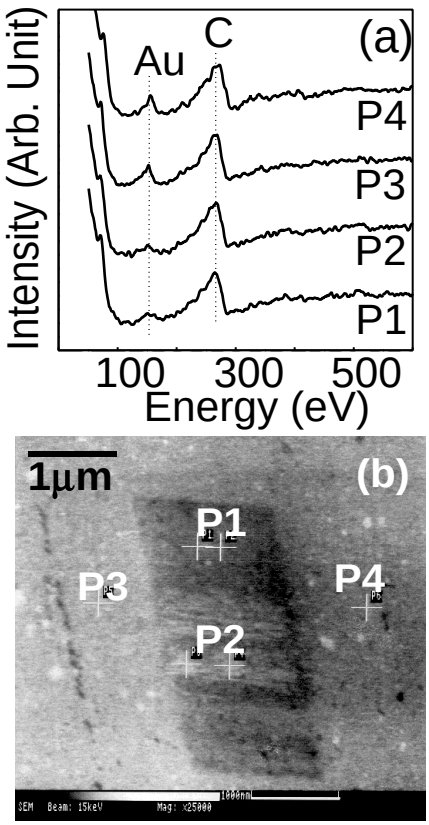

Fig. 4. (a) Auger spectra of P1 and P2 in (a) were obtained from the AFM patterned surface indicated respectively by P1 and P2 in (b). The spectra P3 and P4 in (a) were from the bare Au surface of P3 and P4 in (b). (b) Typical SEM image of an AFM patterned feature on the surface of Au strip.

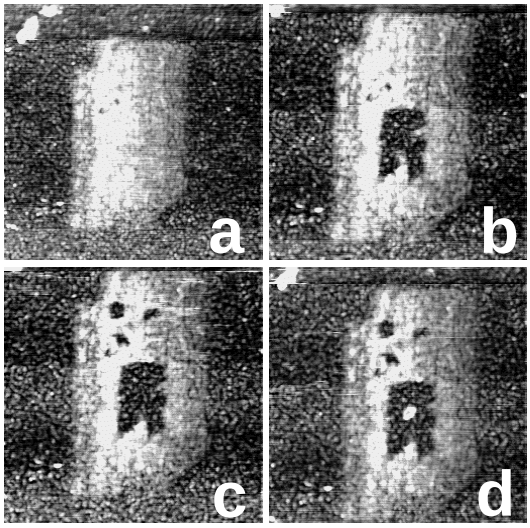

Fig. 5. A typical example of rewritable data storage by the reversible polymerization process: (a) Large area written. (b) Large area erased. (c) Small area erased. (d) Bit rewritten.

is covered by the residuals of the resist and the striping solution, because the surface is not plasma ashed after the liftoff. Therefore, the carbonaceous material on the surface may be originated from the resist or the striping solution instead of what we believe to be the ambient gas molecules.

4. Conclusion

We have demonstrated the controlled writing, erasing and rewriting of nanometer-scale carbon-rich deposits on the surface of gold microstrips using the voltage-biased AFM in air. Chemical analysis of these deposits shows them to be similar to deposits made using electron and ion beams, composed primarily of the carbon species. We think that the reversible patterning demonstrated here is not only applicable for integrated memory and data storage, but also can be employed for a large-scale maskless lithography. In addition, we have introduced the novel AFM nanomachining techniques that may be of interest to making ultra narrow electrodes and gaps in exploratory devices such as a single electron transistor.

1) M. A. McCord and R. F. Pease: J. Vac. Sci. & Technol. B **4** (1986) 86.
2) M. Wendel, H. Lorenz and J. P. Kotthaus: Appl. Phys. Lett. **67** (1995) 3732.
3) H. J. Mamin, P. H. Guethner and D. Rugar: Phys. Rev. Lett. **65** (1990) 2418.
4) Y. Hasegawa, K. Akiyama, M. Ono, S.-J. Kahng, Q. K. Xue and K. Nakayama: Appl. Phys. Lett. **75** (1999) 3668.